Catalysis Today 432 (2024) 114624

Contents lists available at ScienceDirect

Catalysis Today

journal homepage: www.elsevier.com/locate/cattod

Emerging contaminants and pathogenic microorganisms elimination in secondary effluent by graphitic carbon nitride photocatalytic ozonation processes

Eryk Fernandes [a], Pawel Mazierski [b], Magdalena Miodyńska [b], Tomasz Klimczuk [c], Adriana Zaleska-Medynska [b], Joana Oliveira [d], Ana Miguel Matos [d], Rui C. Martins [a], João Gomes [a,*]

[a] University of Coimbra, CERES – Chemical Engineering and Renewable Resources for Sustainability, Department of Chemical Engineering, Faculty of Sciences and Technology, Rua Sílvio Lima, Polo II, Coimbra 3030-790, Portugal
[b] Faculty of Chemistry, Department of Environmental Technology, University of Gdansk, Wita Stwosza 63, Gdańsk 80-308, Poland
[c] Department of Solid State Physics, Faculty of Applied Physics and Mathematics, Gdansk University of Technology, Gdańsk 80-233, Poland
[d] University of Coimbra, CERES – Chemical Engineering and Renewable Resources for Sustainability, Laboratory of Microbiology, Faculty of Pharmacy, Azinhaga de St[a] Comba, Polo III, Coimbra 3000-548, Portugal

ARTICLE INFO

Keywords:
Photocatalysis
Escherichia coli
JC virus
Wastewater treatment
Catalyst synthesis
Water reclamation

ABSTRACT

The complexity of water contaminants, both chemical and biological requires an efficient and feasible treatment alternative. Herein, the photocatalytic ozonation treatment using graphitic carbon nitride catalysts was effectively applied for the elimination of a mixture of targeted chemical contaminants, and both *Escherichia coli* bacteria and Human polyomavirus JC (JC virus) in real secondary wastewater. The exfoliation treatment was compared in catalysts prepared using urea and melamine as precursors. The physical treatment provided no significant enhancement in the urea-based catalyst, while the improvement in the structure of the melamine-based (36MCN) material and formation of melem heterojunction increased its catalytic properties. In both sets of contaminants, the photocatalytic ozonation systems were superior to photolytic ozonation, especially regarding ozone consumption. The best catalyst, 36MCN, resulted in a decrease of 57.5%, 33.0% and 29.0% in the ozone dose required to eliminate chemical, bacteria and virus contaminants, respectively. The hydroxyl radicals were also shown as a key responsible for the pollutant's elimination. The higher radical production and decomposition of ozone are possible indications of the better performance of graphitic carbon nitride photocatalytic ozonation, as an efficient tertiary wastewater alternative.

1. Introduction

The assurance of access to basic and safe water and sanitation is a fundamental right for the human population, as defined by the United Nations (UN), in the Sustainable Development Goal 6. The increasing consumption and discharge of chemical products are an important aggravating factor for the unavailability of appropriate drinking water sources [1,2]. These substances can be incorrectly disposed and/or ineffectively treated in wastewater treatment plants (WWTPs) and reach water bodies.

The contaminants of emerging concern (CECs) are an important group of such pollutants, present in a variety of daily used products and industrial processes, such as pharmaceuticals, personal care products, pesticides, flame retardants, surfactants, etc. These chemicals possess yet limited legislation and monitorization, but present carcinogenic, endocrine disruptive, mutagenic and other hazardous effects [3]. Another aspect of the constant release of CECs, specifically antibiotics and other pharmaceuticals, is the formation of antibiotic resistant bacteria (ARB) and genes (ARG), which may lead to future alarming infection outbreaks [4,5].The development of efficient and feasible tertiary treatment technologies for the elimination of CECs and pathogenic microorganisms is a promising solution to reduce the potential of WWTPs as major sources of water contamination. The Advanced Oxidation Processes (AOPs) are a group of treatments based on the

* Corresponding author.
E-mail address: jgomes@eq.uc.pt (J. Gomes).

https://doi.org/10.1016/j.cattod.2024.114624
Received 20 November 2023; Received in revised form 31 January 2024; Accepted 4 March 2024
Available online 6 March 2024

production of highly oxidative species such hydroxyl (·OH) and other radicals, which are non-selective and capable of achieving high removals of multiple contaminants, both chemical and biological. Photocatalytic systems are an example of such processes and are very adaptable and flexible methods due the variety of catalysts that may be applied, which are materials capable of producing oxidant radicals through photon absorption and consequent chemical reactions.

The selection of the photocatalytic material is a key aspect of the implementation of systems both efficient and economically viable. Graphitic carbon nitride (g-C_3N_4) is a non-metal polymeric catalyst, produced mostly by the simple thermal polymerization of carbon and nitrogen-rich compounds, and are known to possess activity under visible radiation, making its activation under solar radiation possible, and dismissing the use of artificial light sources. Specifically in water disinfection treatments, different g-C_3N_4-based systems have been successfully applied [6–8]. Using a melamine-based g-C_3N_4, Li et al. [9] obtained a 8-log reduction of Bacteriophage MS2 within 6 h under visible-light photocatalysis, demonstrating the capacity of bulk g-C_3N_4 to be applied in the removal of pathogenic microorganisms. The efficiency of carbon nitride catalysts can be further increased through the selection of key parameters in the materials synthesis, as well as posterior modifications of its structure and combinations with other technologies. In our previous studies, the comparison of 3 bulk g-C_3N_4 using different common precursors, melamine, urea and thiourea, was made for the photocatalytic removal of parabens, as known endocrine disruptors [10]. A higher performance of urea-based catalyst was obtained, specially under solar radiation, achieving 92% removals within 3 h, mostly due to its higher surface area. In fact, the low surface area is a common disadvantage of g-C_3N_4 catalysts. The surface area of such materials can also be increased after synthesis, using techniques such as exfoliation. The exfoliation of melamine-based g-C_3N_4 was also previously studied, using alcohol and ultrasound, a simpler alternative method, as usually strong acids are applied [11]. After 36 h of exfoliation, the BET surface area increased from 2.18 $m^2\ g^{-1}$ of the bulk catalyst, to 28.34 $m^2\ g^{-1}$.

The combination of photocatalysis with other AOPs is known to greatly increase the system efficiency, due to synergetic effects. Different systems have been studied using g-C_3N_4 catalyst, and other AOPs, such as Fenton, ozonation and persulfate/peroxymonosulfate [12–17]. The use of photocatalysis and ozonation have been studied using multiple materials, possessing different positive effects. The high performance of ozone as an electron receptor is a great aspect regarding the reduction of the recombination of the photogenerated species by the catalyst, moreover, ozone itself is a highly oxidative species and may directly react with contaminants, or produce other radicals, such as hydroxyls [18]. On the other side, ozone has a low solubility in water, and may rapidly escape from the reaction medium, and the catalyst may contribute by decomposing the ozone and reducing its needed amount and consequent costs. Photocatalytic ozonation under ultraviolet radiation was previously studied using a 36 h exfoliated g-C_3N_4, for the removal of a synthetic mixture of 6 different CECs, and compared to photolytic ozonation, the combined process reduced in around 20% the transferred ozone dose required for the complete elimination of pollutants [11]. Nonetheless, there are few studies regarding the use of ozone and g-C_3N_4 photocatalysis, and further investigation of the different interaction within the system, especially in more complex and real scenarios is needed.

In the present study, different g-C_3N_4 catalyst were compared, regarding its precursor and exfoliation treatment, for the elimination of both chemical and biological contaminants in real secondary wastewater. For the analysis of chemical contaminants elimination, the effluent was spiked with a mixture of 6 pollutants, sulfamethoxazole (SMX), acetaminophen (PCT), carbamazepine (CBZ), methylparaben (MP), ethylparaben (EP) and propylparaben (PP). Microbiological disinfection was investigated regarding *Escherichia coli* bacteria and Human polyomavirus JC (JC virus) present in the secondary wastewater.

2. Materials and methods

2.1. Materials

Sulfamethoxazole (SMX), acetaminophen (PCT), carbamazepine (CBZ), methylparaben (MP), ethylparaben (EP), and propylparaben (PP) were obtained from Sigma-Aldrich. For the evaluation of photocatalytic mechanism, isopropanol (IPA) from Sigma-Aldrich, was used as hydroxyl radical scavenger. Urea and melamine (Thermo Scientific) were used as photocatalyst precursors, and methanol (analytical grade, STANLAB) was applied for catalyst exfoliation.

The secondary wastewater (SWW) (Table 1) was obtained from municipal wastewater treatment plant in the center of Portugal. The WWTP system present a primary settler, activated sludge treatment and secondary settler. The fresh SWW was retrieved in different days, especially to guarantee the presence of microorganisms that would decay in storage. Nonetheless, the initial concentration of *Escherichia coli* was always in the same order, 10^3 CFU mL^{-1}, while JC virus varied from 10^5-10^4 copies L^{-1}.

2.2. Catalyst synthesis

Graphitic carbon nitride was prepared through thermal polymerization of melamine and urea, as previously described [10,11]. Briefly, the precursors were placed in covered crucibles and heated at 550 °C for 4 h. After, the materials were grounded, washed with methanol, and dried. Finally, for the exfoliation treatment, the catalysts were introduced in vials with methanol and set in ultrasound bath for 36 h (800 W, 50 Hz). A list of samples with synthesis details is presented in Table 2.

2.3. Photocatalytic ozonation experiments

The reactions were performed in a 2 L jacketed glass reactor, kept at 25 °C and magnetically stirred at 700 rpm. For the radiation source, 3 UVA Philips TL 6 W BLB lamps (λ_{main}= 365 nm) were used.

For the evaluation of chemical pollutants removal, the secondary wastewater was spiked with a solution containing 1 mg L^{-1} of each SMX, PCT, CBZ, MP, EP and PP. The duration of all reactions was 2 h, the volume treated was 2 L and the catalyst load was 200 mg L^{-1}. Samples were taken during reactions for further analysis.

The ozone was produced from an ozone generator (802 N, BMT) from a pure oxygen stream at 0.2 L min^{-1}, and the inlet and outlet ozone concentration were measured through gas analyzers (BMT 963 and BMT 964). The Transferred Ozone Dose (TOD) was obtained using the following equation:

$$TOD = \int_0^t \left([O_3]_i - [O_3]_o\right) \times \frac{Q_G}{V_L} \quad dt \tag{1}$$

Where $[O_3]_i$ and $[O_3]_o$ are the inlet and outlet ozone concentrations, respectively, in $mg_{O3}\ L^{-1}$, Q_G is the ozone inflow and V_L the volume of

Table 1
Physicochemical and biological properties of the secondary wastewater (SWW).

Parameter	SWW
pH	7.6 ± 0.2
COD ($mgO_2\ L^{-1}$)	43.1 ± 16.8
CBO_5 ($mgO_2\ L^{-1}$)	22.6 ± 1.8
TSS (mg L^{-1})	20.5 ± 7.8
TN (mgN L^{-1})	33.2 ± 3.5
TP (mgP L^{-1})	3.2 ± 0.4
***E. coli* (log CFU mL^{-1})**	3.6 ± 0.2
JC virus (log copies L^{-1})	5.4 ± 0.5

Table 2
Sample labels, BET surface area and energy band gap of prepared catalysts.

Sample label	Type of C_3N_4 precursor	Exfoliation procedure	BET surface area ($m^2\ g^{-1}$)	Energy band gap (eV)
UCN	urea	-	51.27	2.78
36UCN	urea	36 h	57.36	2.77
36MCN	melamine	36 h	28.34	2.75

liquid.

2.4. Analytical techniques

Powder X-ray diffraction analysis was conducted at ambient temperature with a Bruker D8 Focus diffractometer, employing Cu Kα radiation and a LynxEye XE-T detector. The X-ray diffraction data was gathered over a 30-minute duration, scanning from 2θ angles between 2 and 35 degrees. The structural features of catalysts were analyzed using a JEOL JSM-7610 F field-emission scanning electron microscope (FE-SEM). Diffuse reflectance spectra were recorded using a Shimadzu UV 2600 UV-Vis spectrophotometer, which was outfitted with an integrating sphere. The spectrophotometer functioned in the 300–800 nm wavelength range, using $BaSO_4$ as a calibration standard. Additionally, the surface area of the catalysts was quantified employing the Brunauer–Emmelt–Teller (BET) method. BET surface area was measured with a relative pressure range (p/p_0) from 0.05 to 0.3, using a 3 P Instruments' Micro 100 device. The photoluminescence (PL) emission spectra were measured at ambient temperature utilizing a PerkinElmer LS-50B luminescence spectrometer featuring a xenon discharge lamp for illumination and an R928 photomultiplier for detection. The excitation irradiation used for these measurements had a wavelength set at 300 nm.

High-performance liquid chromatography (HPLC) (Waters 2695) was used for the contaminants analysis, using a C18 SiliChrom column at the temperature of 40 ºC. The mobile phase was composed by mixture of methanol and acidified water (0.1% orthophosphoric acid), with a flow of 1 mL min^{-1}.

Total organic carbon (TOC) was determined using a TOC-V CPN model (Shimadzu, Japan) analyzer, and a coupled autosampler model V-ASI (Shimadzu, Japan).

The membrane filtration method was used for *Escherichia coli* quantification tests, according to ISO 9308–1:2014. The collected samples were diluted in order to achieve plate counts below 150 CFU, and tests were performed in duplicate. After virus concentration by ultracentrifugation, JC virus load was accessed through a real-time polymerase chain reaction (PCR) protocol [19].

2.5. Toxicity evaluation

The phytotoxicity of the initial and treated solutions were tested using *Lepidium sativum* seeds. Seeds were dispersed in petri dishes and left in contact with the solutions and kept for 48 h at 27 °C in the dark. The germination index (GI) was calculated according to Trautmann and Krasny [20] criteria.

The luminesce inhibition of *Allivibrio fischeri* bacteria was also used to assess sample's toxicity towards marine species. Samples were inoculated, in duplicates, using the bacteria suspension at 15 ºC in a LUMISTherm (HACH) and LUMIStox 300 equipment from Dr. Lange GmbH (HACH). After 15 min of incubation, the luminescence was directly measured and compared to a NaCl solution (2% wt.) blank control.

3. Results and discussion

3.1. Photocatalysts characterization

The different materials synthesized were characterized using different techniques, to evaluate the impact of exfoliation and precursors in carbon nitride materials production. Fig. 1a displays the pXRD patterns of C_3N_4 catalysts prepared using different methods. The patterns include pristine C_3N_4 synthesized from urea (UCN), as well as two C_3N_4 made using urea and melamine (36MCN) as precursors (36UCN) and subjected to the exfoliation procedure. All catalysts exhibited patterns at 2θ values of approximately 27.3° and 13°. These values align closely with the hexagonal phase of polymeric g-C_3N_4 [21,22]. Furthermore, in the sample labeled 36MCN, which is C_3N_4 derived from melamine and later exposed to the exfoliation process, extra reflections can be noticed, as shown and assigned in Fig. 1a. These are attributed to melem, as previously explained [11,23]. The incorporation of melem has been observed to enhance the activity of C_3N_4 catalysts by formation of heterojunctions [23,24]. However, for C_3N_4 derived from urea and subsequently exfoliated (36UCN), the melem was not detected. This absence might be attributed to the fact that layers produced from urea are notably larger than those derived from melamine, and as a result, undergo the exfoliation process to a minimal degree [10]. Additionally, after intensity normalization, there are no discernible differences between the UCN and 36UCN samples. The UCN diffractogram exhibits a marginally elevated background in the 5–12 degree range. This could potentially be attributed to the presence of an amorphous phase, which seems to be more pronounced in this particular sample.

Fig. 1b displays the DRS UV-Vis spectra for the prepared catalysts, with Tauc's plot presented as an inset. All the catalysts demonstrated comparable photoabsorption characteristics within the measured range. The sample labeled 36MCN exhibited reduced photoabsorption between 300 and 450 nm when compared to catalysts derived from urea. The band gap energy calculated for UCN, 36UCN, and 36MCN were nearly identical, with values of 2.78, 2.77, and 2.75, respectively (Table 2). These values are within the range reported in the literature [25]. The exfoliation of C_3N_4 obtained from urea polycondensation did not alter its optical properties. This suggests that after thermal treatment, the layers became so thin that they remained unaffected by subsequent processes. For C_3N_4 derived from melamine, a distinct pattern emerged. After exfoliation, the energy band gap measured 2.74 eV, whereas for the untreated C_3N_4 from melamine, was stood at 2.6 eV [11]. This change can be ascribed to the enhanced quantum size effect [26].

Fig. 1c displays the photoluminescence (PL) spectra of the synthesized catalysts, exhibiting a peak emission around 460 nm, typical for this kind of materials [27]. Generally, it is observed that a decrease in the intensity of photoluminescence (PL) emission corresponds to a reduced recombination rate of photogenerated electron-hole pairs [28,29]. As illustrated in Fig. 1c, the sample labeled '36 MCN' exhibited the lowest photoluminescence (PL) intensity. This observation suggests that 36MCN demonstrates the most efficient charge recombination process, likely due to the formation of heterojunctions [30].

The findings were further corroborated by the SEM images presented in Fig. 2. along with the measured BET surface area summarized in Table 2. The morphology of C_3N_4 from urea remained almost consistent both before and after the exfoliation process. Each sample displayed a composition of layered structures, characterized by their irregular shapes with dimensions up to several micrometers in size. The layer's thickness reached values less than 50 nm. Similarly, after the exfoliation process, the BET surface showed only a marginal increase from 51.27 to 57.36 $m^2\ g^{-1}$. This indicated that with urea as the precursor of C_3N_4, exfoliation likely reduced the aggregation of layers rather than diminishing their size. For the melamine derived C_3N_4, the BET surface area increased from 2.18 to 28.34 $m^2\ g^{-1}$ after exfoliation which can be attributed to a significant change in layers size [11].

3.2. Chemical contaminants removal

The three produced catalysts were compared in combination with ozone, for the degradation of a spiked solution of SWW, containing a mixture of 6 contaminants (Fig. 3). To better evaluate the synergetic

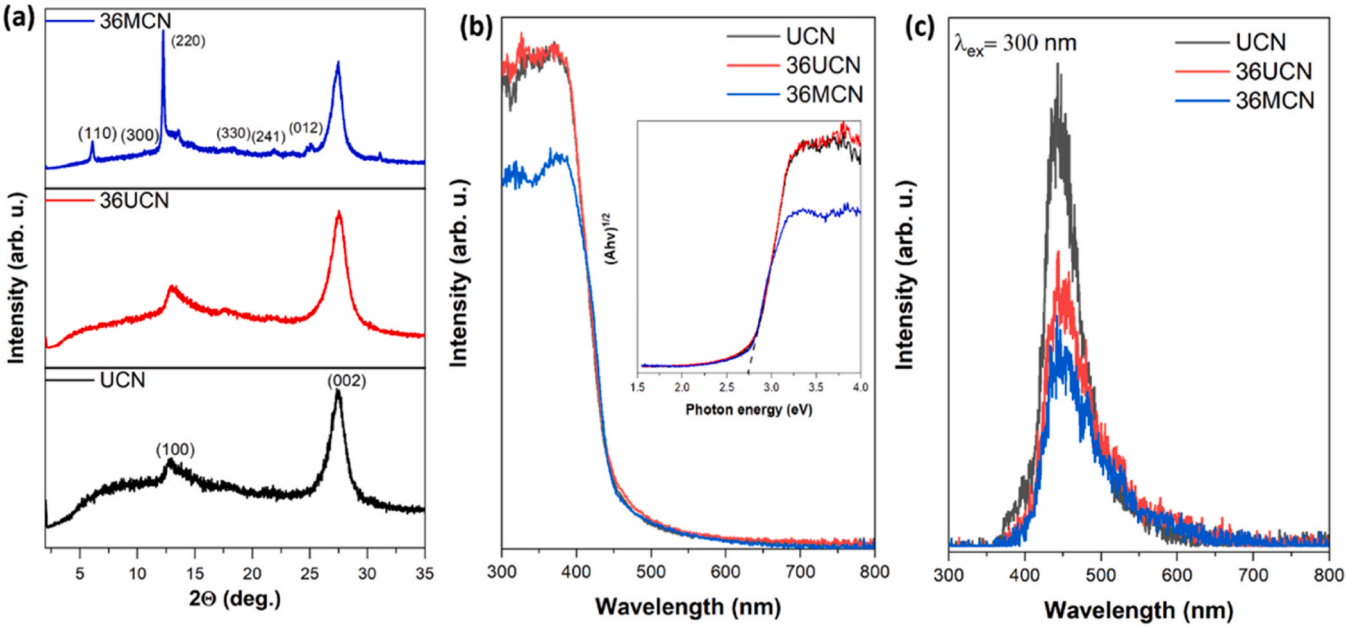

Fig. 1. (a) pXRD patters of prepared catalysts, (b) DRS UV-Vis spectra and Taunc's plot of prepared catalysts, (c) PL emission spectra of prepared catalysts.

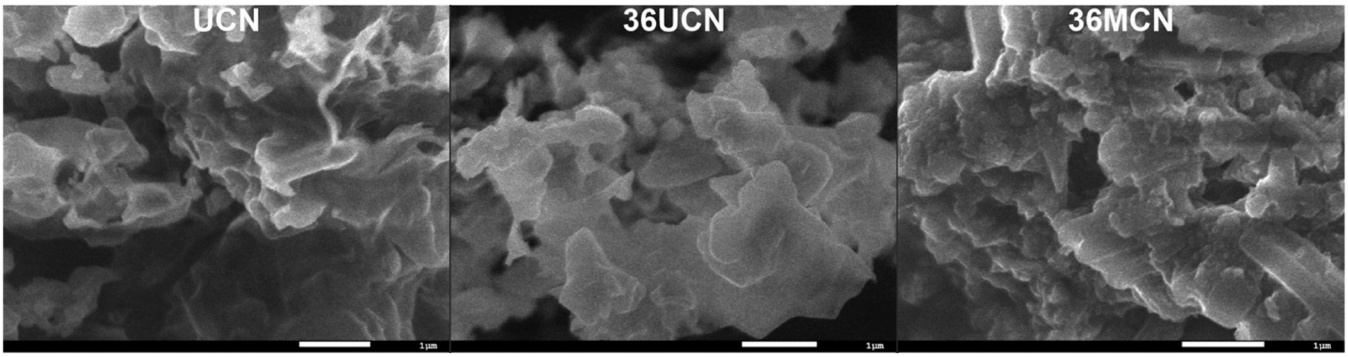

Fig. 2. SEM images of prepared catalysts.

effect between ozonation and photocatalysis, a photolytic ozonation reaction was also conducted. The application of processess using real water matrices is fundamental to elaborate a efficient tertiary treatment alternative, as these mediums are highly complex, possessing different component (i.e. organic matter, Cl^-, SO_4^{2-}, HCO_3^-) that may interfere in the oxidative radicals performance [31].

In the absence of a catalyst, the ozone process was able to achieve a great elimination of the selected contaminants, completely degrading all under 30 min, except for CBZ (93.3%). Single ozonation is a highly efficient process for water treatment, particularly due to the high oxidizing capacity of ozone. The ozone is capable of producing other oxidative radicals through a series of reactions in the medium, or also directly reacts with the organic molecules, specially with compounds possessing high electronic dense structures, such as aromatic rings. Nonetheless, the different tendency of the degradation of carbamazepine might be due to its condensed rings structure, which added to the radical competitivity in the medium containing different molecules and ions, delay its removal. Jesus et al. [32] presented similar results regarding the elimination of CBZ in a spiked SWW during ozonation treatment, not being totally removed under 30 min, while when in a ultrapure solution, it was fully degraded under 10 min. As the reaction occur and other radical scavenging compounds are removed, the rate of elimination of CBZ increases in a later phase of the reaction.

The use of graphitic carbon nitride catalysts in combination with ozone accomplished better performances regarding all three catalysts compared to photolytic ozonation. The presence of the catalyst enhances the production of radicals, both from the actual photoactivation of the material and consequent generation of the photocarriers, but also through the decomposition of ozone. The combined process may also present a higher tendency towards the complete mineralization of pollutants, other than their partial oxidation, forming refractory by-products, which is known disadvantage of ozonation [31,33,34]. These different advantageous factors of photocatalytic ozonation are fundamental to treat water matrices with higher levels of complexity, and achieve a more pure final solution.

The urea-based catalysts produced similar results for the removal of the selected pollutants. Previously, was found that, comparing bulk g-C_3N_4 produced using different precursors, that urea resulted in a catalyst with much larger specific surface are, especially compared to melamine [10]. Thus, as this catalyst already possessed smaller plates and separated layers, the exfoliation treatment have no significant effect. Moreover, the used treatment possibly damaged the catalyst structure, even in a small degree, as found through its characterization.

The melamine-based exfoliated g-C_3N_4 (36MCN) presented a slightly faster decomposition of contaminants, in terms of degradation over time. The ultrasonic treatment is able to rupture some C-NH-C groups that bonds the s-heptazine units, releasing some of the fundamental shorter units that forms the polymeric material, especially melem, that

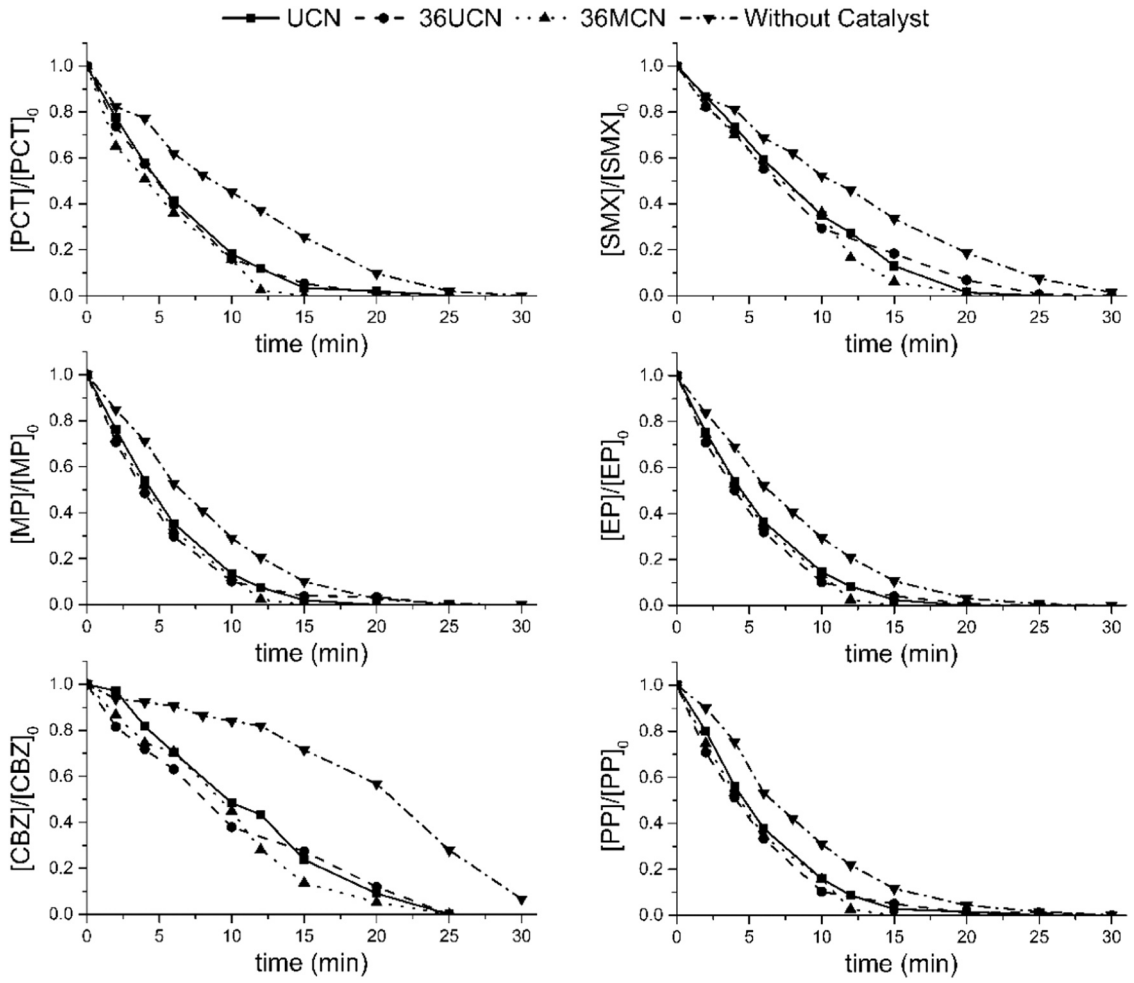

Fig. 3. Photocatalytic ozonation using UCN, 36UCN and 36MCN catalysts, and photolytic ozonation, for the elimination of SMX, PCT, MP, EP, CBZ and PP over time.

may enhance the photocatalytic performance of the g-C_3N_4 [11,24].

The differences between the photocatalytic reactions becomes clearer when analyzed using the transferred ozone dose (Fig. 4). Photolytic ozonation accounted for a TOD of 25.9 mg_{O3} L^{-1} and not fully removed the contaminant, while all photocatalytic reactions presented ozone doses below 20.0 mg L^{-1} for a complete treatment. This lower ozone usage is a result of mainly two factors, the production of oxidative radicals by the catalyst itself, and for the formation of radicals through ozone decomposition [35,36].

The 36MCN resulted in the lowest amount of TOD to obtain a full elimination of the selected CECs, 11.0 mg L^{-1}, which is 44.7%, 39.5% and 57.5% lower than 36UCN, UCN and single ozonation, respectively. The decrease in the ozone usage is a high interest factor for the implementation of treatment process in a larger scale, as the ozone production is associated with high energy costs. Another important parameter to be observed for the further implementation of the process is the loss of mass of the material during synthesis. The urea material presents a very low yield, with mass losses up to 97% during thermal polymerization, compared to 45% when melamine is used, reducing the amount of precursor needed and associated costs.

The study of photocatalytic systems using real wastewater conditions is fundamental to test their efficiencies and the effect of the complexity of different parameters and compounds in these systems. For instance, the presence of organic and inorganic compounds greatly increases the ozone intake. In a previous study, 36MCN photocatalytic ozonation accounted for TOD of 4.9 mg_{O3} L^{-1} for the degradation of the mixture of the 6 selected contaminants in a ultrapure water solution, less than half of the amount needed for the same mixture in a real effluent [11].

To better elucidate the differences for the ozone-based reactions, a kinetic evaluation was made using a pseudo-first order kinetic model based on the transferred ozone doses (Eq. 2), and the rate constants are shown in Table 3.

$$-\ln(C/C_0) = k'_{TOD} \times TOD \quad (2)$$

Through the analysis of the reaction rate constants, it's clear the faster decomposition of the contaminants mixture using the 36MCN catalyst, with values 2–3 times higher than the photolytic reaction, and 19–59% higher than the second-best catalyst, 36UCN. Carbamazepine had the lowest rate constants in all systems, possibly due to the difficulty of radicals to attack its condensed structure, as previously said. The more branched chemicals possess structures more susceptible to the radicals' attack, thus present higher rate constants.

Jesus et al. [32] investigated the single ozonation treatment of a mixture of PCT, SMX, CBZ, MP and PP, and the determined pseudo-first order reaction rate constants based upon TOD values follows a similar pattern of the values obtained herein, with SMX and CBZ presenting lower rate constants compared to the other contaminants. The second-order rate constants obtained by Tay et al. [37] for MP, EP and PP for ozone (k_{O3}) are respectively 2.5, 3.4 and 4.1 $\times 10^5$ M^{-1} s^{-1} at pH 6, and for hydroxyl radical ($k_{\cdot OH}$), 6.8, 7.7 and 8.6 $\times 10^9$ M^{-1} s^{-1}, indicating the important contribution of ·OH for contaminants removal. The PCT, SMX and CBZ constants determined by Hamdi et al. [38] and Koo et al. [39] were similar to parabens, respectively 2.6 $\times 10^6$, 5.7 $\times 10^5$ and 3.0 $\times 10^5$ M^{-1} s^{-1} for k_{O3} and 4.9 $\times 10^9$, 5.5 $\times 10^9$ and 8.8 $\times 10^9$ M^{-1} s^{-1} for $k_{\cdot OH}$. Regarding these second-rate constants, the values were obtained using ultrapure water solutions of single contaminants, thus

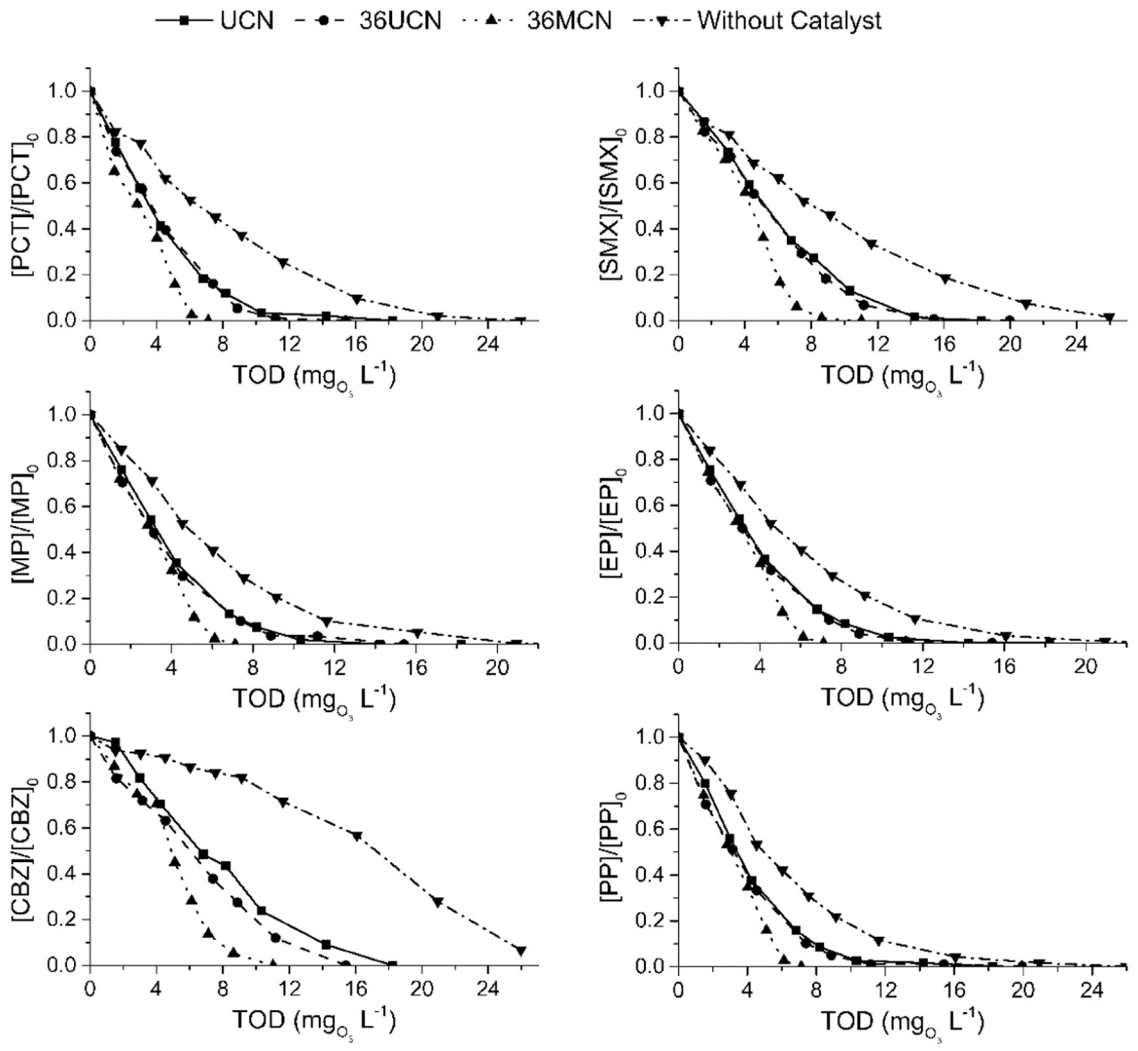

Fig. 4. Photocatalytic ozonation using UCN, 36UCN and 36MCN catalysts, and photolytic ozonation, for the elimination of SMX, PCT, MP, EP, CBZ and PP over the transferred ozone dose (TOD).

Table 3
Pseudo-first order reaction rate constants (L mg_{O3}^{-1}) and R^2 for the ozone-based treatments.

	PCT		SMX		CBZ		MP		EP		PP	
	k'_{TOD}	R^2	k'_{TOD}	R^2	k'_{TOD}	R^2	k'_{TOD}	R^2	k'_{TOD}	R^2	k'_{TOD}	R^2
UCN	0.277	0.98	0.228	0.91	0.139	0.95	0.330	0.97	0.314	0.98	0.299	0.98
36UCN	0.335	0.94	0.255	0.92	0.157	0.96	0.316	0.98	0.368	0.97	0.322	0.97
36MCN	0.432	0.96	0.369	0.95	0.251	0.97	0.454	0.98	0.436	0.97	0.424	0.96
Without Catalyst	0.151	0.95	0.129	0.94	0.067	0.89	0.216	0.95	0.210	0.98	0.186	0.99

the kinetic estimation herein for the mixture in a real effluent is affected by the other compounds present. In real wastewaters, there are multiple organic and inorganic compounds that may interfere in the photocatalytic degradation, as well as the other contaminants added to the mixture, and these interferences, as indicated in other studies, may affect in a higher degree more electrophilic pollutants, resulting in the lower reaction rates for CBZ and SMX compared to the other contaminants [32].

The total organic carbon (TOC) was analyzed for the final treated solutions of all systems studied, with the initial solution having a TOC of 18.68 mg L^{-1}. The single ozonation reaction presented the lowest removal, 17.5%, due to the known tendency of ozone treatment to lead to the formation of refractory by-products. The use of 36MCN catalyst led to the lowest TOC value, 9.74 mg L^{-1}, a 47.9% removal, followed by UCN and 36UCN, with 10.03 and 10.20 mg L^{-1}. The combination of photocatalysis and ozonation improve the mineralization route of chemicals degradation, other than partial oxidation, leading to the

Table 4
Allivibrio fischeri luminescence inhibition and Lepidium sativum germination index prior and after ozone-based treatments.

	Luminescence inhibition after 15 min (%)	Germination Index (%)
Spiked Solution	48.29	61.4
Bulk Urea (UCN)	32.77	37.3
Exfoliated Urea (36UCN)	32.67	59.1
Exfoliated Melamine (36MCN)	25.74	64.8
Without Catalyst	32.64	52.6

formation of CO_2 and H_2O.

The toxicity prior and after treatment was also tested (Table 4). The luminescence inhibition of *A. fischeri* bacteria considerably decreased after all treatments, achieving its minimal value when 36MCN catalyst was used. The toxicity towards this bacteria is a key parameter to evaluate the effect of the treated solutions to marine life, and values below 30% may be considered non-toxic [40].

The germination index of *L. sativum* seeds when in contact with the initial spiked effluent solution is higher than most of treated solution, except for 36MCN treatment. This may be a result of toxic by-products formed during reaction, that may possess a higher toxicity than the initial pollutants towards this specie. This parameter is interesting to be evaluated due to the possibility of the use of the treated secondary effluent for agricultural irrigation, which is currently highly discussed as water reclamation alternative.

The formation of a treatment system that is efficient regarding different factors is fundamental for future water reclamation and environmental remediation. The decrease in ozone consumption, meaning a lower operating cost, minimal by-products formation, lower toxicity and the simplicity of catalyst synthesis are great advantages of the use of carbon nitride catalysts and ozonation [41]. Nonetheless, the process may be further improved to overpass other application drawbacks of this type of technology. Catalyst doping is a known technique to boost catalytic activity, introducing foreign elements in the catalyst structure that may introduce photogenerated species trapping sites and defect states, narrowing the bandgap and reducing recombination, and even improve O_3 adsorption over the catalyst surface [12,42,43]. Moreover, composite formation, combining different materials with carbon nitride, may also be explored to enhance the catalyst, not only its photocatalytic properties, but also typical photocatalyst drawbacks, such as the catalyst separation after treatment [44–46].

3.3. Pathogens disinfection

The exfoliated MCN catalyst was also employed in preliminary studies for the disinfection of secondary wastewater, targeting the removal of enterobacteria *Escherichia coli*. The evolution of the disinfection reaction was compared over the transferred ozone dose (Fig. 5), as the main objective is to evaluate photolytic and photocatalytic ozonation systems, and it allows a superior and clearer comparison. Nonetheless, over the time, the observed behavior of the reactions was similar.

The photo-ozone systems are proven efficient technologies for water disinfection, and currently employed in drinking water treatment plants [47,48]. The main advantage of the ozone-based process is the short time contact needed for the microorganism's disinfection. Nevertheless, the high energy demand, which may comprehend for 26–43% of the total costs of the system, and even that there are no chlorinated by-products formed as other common drinking water treatments, studies shown that other harmful compounds may be formed, such as NDMA [47].

The ozone consumption for the elimination of *E. coli* was considerably lower in the photocatalytic ozonation process compared to single photolytic ozonation, with a final TOD to obtain a complete disinfection of 20.2 mg L^{-1} and 29.8 mg L^{-1} respectively. This result is in agreement with the improved performance of the photocatalytic ozonation treatment found during chemical contaminants elimination, and further highlight its benefits.

To evaluate the contribution of hydroxyl radicals in the *E. coli* removal, 10 mM of isopropanol (IPA) was used in a reaction as a radical scavenger (Fig. 5). The disinfection treatment in the presence of IPA didn't achieve a complete elimination of *E. coli*, and also demonstrated a higher consumption of ozone. The ·OH radicals are one of the major reactive oxygen species (ROS) responsible for the bacterial inactivation, able to damage their cell wall and membranes [6]. In the absence of the ·OH, other radicals, such as superoxide and molecular ozone, play major roles in the bacterial elimination, which reflects on the higher ozone consumption.

The kinetics evaluation of the disinfection treatments based on the TOD values was also conducted. There are more complex models that are appointed to better evaluate the disinfection kinetics of ozone systems, such as logistic models, but typically are based upon multiple empirical constants and complex calculations, that usually are not precisely described [49]. For an initial evaluation, the first-order disinfection model (Eq. 3) was taken as good approximation (R^2>0.92), even with some linear deviations due to ozone instability.

$$-\ln(N/N_0) = k'_{TOD} \times TOD \quad (3)$$

The photocatalytic ozonation presented the highest reaction rate constant, 0.372 L mg_{O3}^{-1}, almost 2 times compared to photolytic ozonation, 0.206 L mg_{O3}^{-1}. These values corroborate the better performance of photocatalytic ozonation, as a more non-selective and efficient water treatment technology.

The removal of JC virus was also analyzed for the photocatalytic and photolytic ozonation reactions according to the transferred ozone doses (Fig. 6). As the effluent was retrieved in different days, there is a difference by approximately 1 log between the initial virus copies

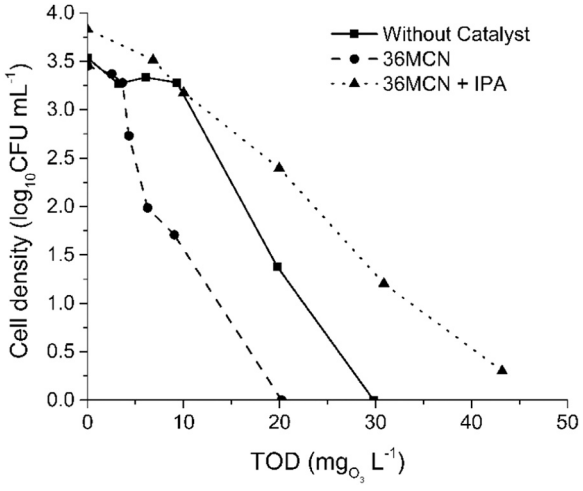

Fig. 5. Photolytic and photocatalytic ozonation treatments for the disinfection of secondary wastewater, using 36MCN catalyst and in the presence of isopropanol (IPA).

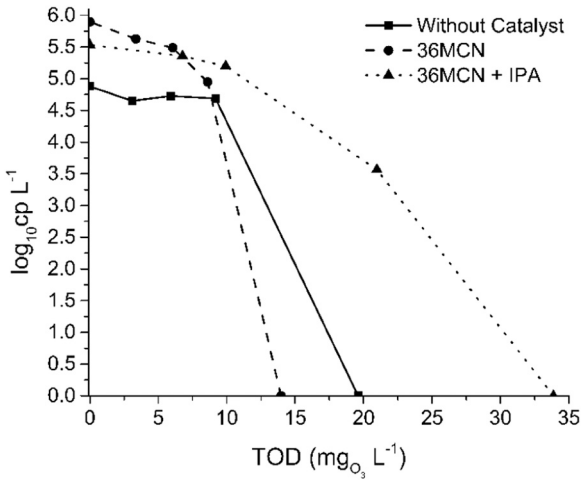

Fig. 6. Photolytic and photocatalytic ozonation treatments for the virus removal of secondary wastewater, using 36MCN catalyst and in the presence of isopropanol (IPA).

concentration for the photocatalytic and photolytic tests.

The virus structure is more resistant to the attack of ozone, compared to *E.* coli, requiring a higher concentration of ozone to obtain a response [19]. Nonetheless, in the removal of the JC virus in the 36MCN photocatalytic ozone system it's possible to observe a faster response of the treatment, with a noticeable variation in its concentration in the first minutes of the reaction, with less than 5 mg L^{-1} of TOD. Comparatively, the single ozonation reaction only demonstrated a significant effect for an ozone concentration higher than 11 mg L^{-1} (15 min). Regarding the time necessary to fully eliminate JC virus from the wastewater, both photolytic and catalytic systems achieved it in 30 min, while the final TOD values were, respectively, 19.6 and 13.9 mg L^{-1}.

The use of isopropanol to block hydroxyl radicals resulted in a severe increase in both time, 45 min, and transferred ozone dose required, 33.87 mg L^{-1}. This results greatly demonstrate the importance of this radical in the elimination of JC virus, at an even higher degree than the observed results for *E. coli* virus. As conducted with the bacteria results, the disinfection kinetics was estimated using Eq. 2, with good correlations for a preliminary result (R^2=0.91–0.95). The reaction rate constants obtained reflects greatly the faster response of the photocatalytic treatment, even with a higher initial viral concentration, 0.218 L mg_{O3}^{-1}, almost 4 times higher than the single ozonation treatment, 0.055 L mg_{O3}^{-1}.

JC virus is widely present in municipal wastewaters, and its pathogenicity is particularly related to individuals under immunodeficiency states, such as bone marrow transplant patients and HIV infection [19]. This virus has been taken a potential indicator of wastewater quality, and there is a great necessity of a feasible tertiary wastewater treatment technology able to inactivate a large variety of pathogenic microorganisms [50].

4. Conclusions

The use of an exfoliation treatment for g-C_3N_4 using different precursors was successfully evaluated. The exfoliation step for the urea-based catalyst produced no significant effects, possibly due to its already thin and more dispersed layers, which was attest by SEM characterization.

The catalysts were all applied in photocatalytic ozonation treatments for the elimination of chemical and biological contaminants in a secondary wastewater. A complete elimination was found for all 6 contaminants targeted for almost all ozone-based systems, and the addition of the synthesized graphitic carbon nitride catalysts produced significant improvements, especially regarding ozone consumption. The 36 h exfoliated melamine-based g-C_3N_4 presented the best results, possibly due to the existence of melem in the catalyst structure and a higher photocarriers separation, even with a surface area considerably lower than the urea catalyst. The great performance of the 36MCN is an indicative of its promising application in water treatment, with good efficiencies in more complex water matrices such as real secondary effluents.

The 36MCN catalyst was also used for the elimination of *Escherichia coli* and JC virus. The photocatalytic ozonation system was proved to be more efficient as a disinfection treatment, with a 33% and 29% lower ozone consumption than the photolytic ozonation for, respectively, bacteria and virus elimination, and consequently reducing its overall costs. The hydroxyl radicals were proved to be a key specie in pathogens elimination, especially for JC virus disinfection, with an ozone requirement almost 3 times higher when this radical was blocked.

Ultimately, the study highlights the efficacy of carbon nitride in photocatalytic ozonation as a promising tertiary treatment alternative. Nonetheless, the effect of the different anions and other compounds that interfere in the reaction, as well as its final separation, which is a known hindrance of photocatalytic systems, still needs to be further studied.

CRediT authorship contribution statement

Tomasz Klimczuk: Visualization, Resources, Methodology. **Joana Oliveira:** Visualization, Methodology, Investigation. **Adriana Zaleska-Medynska:** Writing – review & editing, Resources. **Rui C. Martins:** Writing – review & editing, Visualization, Supervision, Resources, Methodology, Funding acquisition, Conceptualization. **Ana Miguel Matos:** Resources, Methodology, Investigation, Conceptualization. **João Gomes:** Writing – review & editing, Visualization, Supervision, Resources, Methodology, Funding acquisition, Conceptualization. **Eryk Fernandes:** Writing – original draft, Visualization, Methodology, Investigation, Funding acquisition, Conceptualization. **Magdalena Miodyńska:** Visualization, Resources, Methodology. **Pawel Mazierski:** Writing – review & editing, Visualization, Resources, Methodology.

Declaration of Competing Interest

The authors declare that they have no known competing financial interests or personal relationships that could have appeared to influence the work reported in this paper.

Data availability

The authors do not have permission to share data.

Acknowledgements

This Special Issue is dedicated to honor the retirement of Prof. Santiago Esplugas at the Universidad de Barcelona (UB, Spain), a key figure in the area of Catalytic Advanced Oxidation Processes. Prof. Santiago Esplugas was supervisor of Rui C. Martins during his stay at the University of Barcelona has a Post-Doc. This was a very fruitful cooperation since it was his first international experience which opened the doors for many more cooperation's within the area of the AOPs.

Funded by the European Union, under the Grant Agreement GA101081953 attributed to the project H_2O for All—Innovative Integrated Tools and Technologies to Protect and Treat Drinking Water from Disinfection Byproducts (DBPs). Views and opinions expressed are, however, those of the author(s) only and do not necessarily reflect those of the European Union. Neither the European Union nor the granting authority can be held responsible for them.

The authors gratefully acknowledge FCT (Fundação para a Ciência e Tecnologia, Portugal) for the Ph.D. Grant (2020.06130.BD) and the financial support (CEECIND/01207/2018). Thanks are due to FCT/MCTES for the financial support to CIEPQPF/CERES (UIDB/00102/2020).

References

[1] N. Delgado, J. Orozco, S. Zambrano, J.C. Casas-Zapata, D. Marino, Veterinary pharmaceutical as emerging contaminants in wastewater and surface water: an overview, J. Hazard. Mater. 460 (2023), https://doi.org/10.1016/j.jhazmat.2023.132431.

[2] E. Ben Mordechay, M. Shenker, J. Tarchitzky, V. Mordehay, Y. Elisar, Y. Maor, J. J. Ortega-Calvo, D. Hennecke, T. Polubesova, B. Chefetz, Wastewater-derived contaminants of emerging concern: concentrations in soil solution under simulated irrigation scenarios, Soil Environ. Heal. 1 (2023) 100036, https://doi.org/10.1016/j.seh.2023.100036.

[3] T.L. Botha, E. Bamuza-Pemu, A. Roopnarain, Z. Ncube, G. De Nysschen, B. Ndaba, N. Mokgalaka, M. Bello-Akinosho, R. Adeleke, A. Mushwana, M. van der Laan, P. Mphahlele, F. Vilakazi, P. Jaca, E. Ubomba-Jaswa, Development of a GIS-based knowledge hub for contaminants of emerging concern in South African water resources using open-source software: lessons learnt, Heliyon 9 (2023) e13007, https://doi.org/10.1016/j.heliyon.2023.e13007.

[4] S. van Hamelsveld, F. Jamali-Behnam, I. Alderton, B. Kurenbach, A.W. McCabe, B. R. Palmer, M.J. Gutiérrez-Ginés, L. Weaver, J. Horswell, L.A. Tremblay, J. A. Heinemann, Effects of selected emerging contaminants found in wastewater on antimicrobial resistance and horizontal gene transfer, Emerg. Contam. 9 (2023), https://doi.org/10.1016/j.emcon.2023.100257.

[5] B.E. Igere, A.I. Okoh, U.U. Nwodo, Lethality of resistant/virulent environmental vibrio cholerae in wastewater release: an evidence of emerging virulent/antibiotic-

resistant-bacteria contaminants of public health concern, Environ. Chall. 7 (2022) 100504, https://doi.org/10.1016/j.envc.2022.100504.
[6] W. Wang, C. Zhou, Y. Yang, G. Zeng, C. Zhang, Y. Zhou, J. Yang, D. Huang, H. Wang, W. Xiong, X. Li, Y. Fu, Z. Wang, Q. He, M. Jia, H. Luo, Carbon nitride based photocatalysts for solar photocatalytic disinfection, can we go further? Chem. Eng. J. 404 (2021) 126540 https://doi.org/10.1016/j.cej.2020.126540.
[7] Y. Ni, M. Wang, L. Liu, M. Li, S. Hu, J. Lin, J. Sun, T. Yue, M. Zhu, J. Wang, Efficient and reusable photocatalytic river water disinfection by addictive graphitic carbon nitride / magnesium oxide nano-onions with particular " nano-magnifying glass effect, J. Hazard. Mater. 439 (2022) 129533, https://doi.org/10.1016/j.jhazmat.2022.129533.
[8] X. Li, G. Huang, Y. Li, X. Chen, Y. Yao, Y. Liang, Low-Cost ceramic disk filters coated with Graphitic carbon nitride (g-C_3N_4) for drinking water disinfection and purification, Sep. Purif. Technol. 292 (2022) 120999, https://doi.org/10.1016/j.seppur.2022.120999.
[9] Y. Li, C. Zhang, D. Shuai, S. Naraginti, D. Wang, W. Zhang, Visible-light-driven photocatalytic inactivation of MS2 by metal-free g-C_3N_4: virucidal performance and mechanism, Water Res 106 (2016) 249–258, https://doi.org/10.1016/j.watres.2016.10.009.
[10] E. Fernandes, P. Mazierski, T. Klimczuk, A. Zaleska-medynska, R.C. Martins, g-C_3N_4 for photocatalytic degradation of parabens: precursors influence, the radiation source and simultaneous ozonation evaluation, Catalysts 13 (2023) 789, https://doi.org/10.3390/catal13050789.
[11] E. Fernandes, P. Mazierski, M. Miodyńska, T. Klimczuk, M. Pawlyta, A. Zaleska-medynska, R.C. Martins, J. Gomes, Carbon nitride exfoliation for photocatalysis and photocatalytic ozonation over emerging contaminants abatement, J. Environ. Chem. Eng. 11 (2023), https://doi.org/10.1016/j.jece.2023.110554.
[12] F. Zhao, Y. Yang, S. Ji, R. Yu, X. Li, Z. Zhou, Photocatalysis-Fenton mechanism of rGO-enhanced Fe-doped carbon nitride with boosted degradation performance towards rhodamine B, J. Water Process Eng. 55 (2023) 104080, https://doi.org/10.1016/j.jwpe.2023.104080.
[13] J. Yue, H. Yang, C. Liu, Q. Zhang, Y. Ao, Constructing photocatalysis-self-Fenton system over a defective twin C_3N_4: in-situ producing H_2O_2 and mineralizing organic pollutants, Appl. Catal. B Environ. 331 (2023) 122716, https://doi.org/10.1016/j.apcatb.2023.122716.
[14] D. Guo, Y. Wang, C. Chen, J. He, M. Zhu, J. Chen, C. Zhang, A multi-structural carbon nitride co-modified by Co, S to dramatically enhance mineralization of Bisphenol f in the photocatalysis-PMS oxidation coupling system, Chem. Eng. J. 422 (2021) 130035, https://doi.org/10.1016/j.cej.2021.130035.
[15] J. Tan, Z. Li, J. Li, J. Wu, X. Yao, T. Zhang, Graphitic carbon nitride-based materials in activating persulfate for aqueous organic pollutants degradation: a review on materials design and mechanisms, Chemosphere 262 (2021) 127675, https://doi.org/10.1016/j.chemosphere.2020.127675.
[16] C.A. Orge, M.J. Sampaio, J.L. Faria, M.F.R. Pereira, C.G. Silva, Efficiency and stability of metal-free carbon nitride in the photocatalytic ozonation of oxamic acid under visible light, J. Environ. Chem. Eng. 8 (2020) 104172, https://doi.org/10.1016/j.jece.2020.104172.
[17] H. Sun, N. Jiang, G. Yu, J. Li, Catalytic ozonation of dissolved acetaminophen with iron-doped graphitic carbon nitride in plasma-liquid system, Chem. Eng. J. 475 (2023) 146014, https://doi.org/10.1016/j.cej.2023.146014.
[18] J. Xiao, Y. Xie, H. Cao, Organic pollutants removal in wastewater by heterogeneous photocatalytic ozonation, Chemosphere 121 (2015) 1–17, https://doi.org/10.1016/j.chemosphere.2014.10.072.
[19] J. Gomes, D. Frasson, R.M. Quinta-Ferreira, A. Matos, R.C. Martins, Removal of enteric pathogens from real wastewater using single and catalytic ozonation, Water 11 (1) (2019) 12, https://doi.org/10.3390/w11010127.
[20] N.M. Trautmann, M.E. Krasny, Composting in the classroom, New York, 1997.
[21] T. Cao, M. Cai, L. Jin, X. Wang, J. Yu, Y. Chen, L. Dai, Amorphous Cr-doped g-C_3N_4 as an efficient catalyst for the direct hydroxylation of benzene to phenol, New J. Chem. 43 (2019) 16169–16175, https://doi.org/10.1039/c9nj03483h.
[22] C. Zhang, J. Liu, X. Huang, D. Chen, S. Xu, Multistage polymerization design for g-C_3N_4 nanosheets with enhanced photocatalytic activity by modifying the polymerization process of melamine, ACS Omega 4 (2019) 17148–17159, https://doi.org/10.1021/acsomega.9b01510.
[23] J. Mo, N. Wang, S. Zhang, X. Chen, J. Fu, P. Chen, Z. Liang, Q. Su, X. Li, Metal-free g-C3N4/melem nanorods hybrids for photocatalytic degradation of methyl orange, Res. Chem. Intermed. 48 (2022) 3835–3849, https://doi.org/10.1007/s11164-022-04779-6.
[24] M. Michalska, V. Matějka, J. Pavlovský, P. Praus, M. Ritz, J. Serenčíšová, L. Gembalová, M. Kormunda, K. Foniok, M. Reli, G. Simha Martynková, Effect of Ag modification on TiO_2 and melem/g-C3N4 composite on photocatalytic performances, Sci. Rep. 13 (2023) 1–20, https://doi.org/10.1038/s41598-023-32094-6.
[25] R.C. Sahoo, H. Lu, D. Garg, Z. Yin, H.S.S.R. Matte, Bandgap engineered g-C_3N_4 and its graphene composites for stable photoreduction of CO_2 to methanol, Carbon N. Y 192 (2022) 101–108, https://doi.org/10.1016/j.carbon.2022.02.021.
[26] S. Yang, Y. Gong, J. Zhang, L. Zhan, L. Ma, Z. Fang, R. Vajtai, X. Wang, P. M. Ajayan, Exfoliated graphitic carbon nitride nanosheets as efficient catalysts for hydrogen evolution under visible light, Adv. Mater. 25 (2013) 2452–2456, https://doi.org/10.1002/adma.201204453.
[27] J. Xue, S. Ma, Y. Zhou, Z. Zhang, M. He, Facile photochemical synthesis of Au/Pt/g-C_3N_4 with plasmon-enhanced photocatalytic activity for antibiotic degradation, ACS Appl. Mater. Interfaces 7 (2015) 9630–9637, https://doi.org/10.1021/acsami.5b01212.
[28] H.T. Ren, S.Y. Jia, Y. Wu, S.H. Wu, T.H. Zhang, X. Han, Improved photochemical reactivities of Ag_2O/g-C_3N_4 in phenol degradation under UV and visible light, Ind. Eng. Chem. Res. 53 (2014) 17645–17653, https://doi.org/10.1021/ie503312x.
[29] W. Sun, Z. Fu, H. Shi, C. Jin, E. Liu, X. Zhang, J. Fan, Cu_3P and Ni_2P co-modified g-C_3N_4 nanosheet with excellent photocatalytic H2 evolution activities, J. Chem. Technol. Biotechnol. 95 (2020) 3117–3125, https://doi.org/10.1002/jctb.6487.
[30] C. Huang, S. Zhang, M. Wang, H. Xu, M. Li, B. Song, G. Shao, H. Wang, H. Lu, R. Zhang, Construction of melem/g-C_3N_4/vermiculite hybrid photocatalyst with sandwich structure, Appl. Clay Sci. 213 (2021) 106242, https://doi.org/10.1016/j.clay.2021.106242.
[31] E. Fernandes, R.C. Martins, J. Gomes, Photocatalytic ozonation of parabens mixture using 10% N-TiO_2 and the effect of water matrix, Sci. Total Environ. 718 (2020) 137321, https://doi.org/10.1016/j.scitotenv.2020.137321.
[32] F. Jesus, E. Domingues, C. Bernardo, J.L. Pereira, R.C. Martins, J. Gomes, Ozonation of selected pharmaceutical and personal care products in secondary effluent—degradation kinetics and environmental assessment, Toxics 10 (2022) 765.
[33] M.Z. Fidelis, Y.B. Favaro, A.S.G.G. dos Santos, M.F.R. Pereira, R. Brackmann, G. G. Lenzi, O.S.G.P. Soares, O.A.B. Andreo, Enhancing Ibuprofen and 4-Isobutylacetophenone degradation: exploiting the potential of Nb_2O_5 sol-gel catalysts in photocatalysis, catalytic ozonation, and photocatalytic ozonation, J. Environ. Chem. Eng. 11 (2023), https://doi.org/10.1016/j.jece.2023.110690.
[34] E. Mena, A. Rey, S. Contreras, F.J. Beltrán, Visible light photocatalytic ozonation of DEET in the presence of different forms of WO_3, Catal. Today 252 (2015) 100–106, https://doi.org/10.1016/j.cattod.2014.09.022.
[35] J.F. Gomes, K. Bednarczyk, M. Gmurek, M. Stelmachowski, A. Zaleska-Medynska, F.C. Bastos, M.E. Quinta-Ferreira, R. Costa, R.M. Quinta-Ferreira, R.C. Martins, Noble metal–TiO_2 supported catalysts for the catalytic ozonation of parabens mixtures, Process Saf. Environ. Prot. 111 (2017) 148–159, https://doi.org/10.1016/j.psep.2017.07.001.
[36] B. Liu, M. Zhang, J. Yang, M. Zhu, Efficient ozone decomposition over bifunctional Co_3Mn-layered double hydroxide with strong electronic interaction, Chin. Chem. Lett. 33 (2022) 4679–4682, https://doi.org/10.1016/j.cclet.2022.01.025.
[37] K.S. Tay, N.A. Rahman, M.R.Bin Abas, Ozonation of parabens in aqueous solution: kinetics and mechanism of degradation, Chemosphere 81 (2010) 1446–1453, https://doi.org/10.1016/j.chemosphere.2010.09.004.
[38] N. Hamdi El Najjar, A. Touffet, M. Deborde, R. Journel, N. Karpel Vel Leitner, Kinetics of paracetamol oxidation by ozone and hydroxyl radicals, formation of transformation products and toxicity, Sep. Purif. Technol. 136 (2014) 137–143, https://doi.org/10.1016/j.seppur.2014.09.004.
[39] J.W. Koo, J. Lee, S.H. Nam, H. Kye, E. Kim, H. Kim, Y. Lee, T.M. Hwang, Evaluation of the prediction of micropollutant elimination during bromide ion-containing industrial wastewater ozonation using the ROH, O_3 value, Chemosphere 338 (2023) 139450, https://doi.org/10.1016/j.chemosphere.2023.139450.
[40] S. Miralles-Cuevas, I. Oller, A. Agüera, J.A. Sánchez Pérez, S. Malato, Strategies for reducing cost by using solar photo-Fenton treatment combined with nanofiltration to remove microcontaminants in real municipal effluents: toxicity and economic assessment, Chem. Eng. J. 318 (2017) 161–170, https://doi.org/10.1016/j.cej.2016.06.031.
[41] J. Xiao, Y. Xie, J. Rabeah, A. Brückner, H. Cao, Visible-light photocatalytic ozonation using graphitic C_3N_4 catalysts: a hydroxyl radical manufacturer for wastewater treatment, Acc. Chem. Res. 53 (2020) 1024–1033, https://doi.org/10.1021/acs.accounts.9b00624.
[42] I. Idrees, A. Razzaq, M. Zafar, A. Umer, F. Mustafa, F. Rehman, W. Young, Silver (Ag) doped graphitic carbon nitride (g-C_3N_4) photocatalyst for enhanced degradation of Ciprofloxacin (CIP) under visible light irradiation, Arab. J. Chem. 17 (2024) 105615, https://doi.org/10.1016/j.arabjc.2024.105615.
[43] B. Zhu, G. Jiang, S. Chen, F. Liu, Y. Wang, C. Zhao, Multifunctional Cl-S double-doped carbon nitride nanotube unit in catalytic ozone oxidation synergistic photocatalytic system: generation of ROS-rich region and effective treatment of organic wastewater, Chem. Eng. J. 430 (2022) 132843, https://doi.org/10.1016/j.cej.2021.132843.
[44] R. Bayan, N. Karak, Bio-based hyperbranched polymer-supported oxygeneous graphitic-carbon nitride dot as heterogeneous metal-free solar light photocatalyst for oxidation and reduction reactions, Appl. Surf. Sci. 514 (2020) 145909, https://doi.org/10.1016/j.apsusc.2020.145909.
[45] M. Mahdavi, M. Mirmohammadi, M. Baghdadi, S. Mahpishanian, Visible light photocatalytic degradation and pretreatment of lignin using magnetic graphitic carbon nitride for enhancing methane production in anaerobic digestion, Fuel 318 (2022) 123600, https://doi.org/10.1016/j.fuel.2022.123600.
[46] M. Jourshabani, J.A. Dominic, G. Achari, Z. Shariatinia, Synergetic photocatalytic ozonation using modified graphitic carbon nitride for treatment of emerging contaminants under UVC, UVA and visible irradiation, Chem. Eng. Sci. 209 (2019) 115181, https://doi.org/10.1016/j.ces.2019.115181.
[47] M.C. Collivignarelli, A. Abbà, I. Benigna, S. Sorlini, V. Torretta, Overview of the main disinfection processes for wastewater and drinking water treatment plants, Sustainability 10 (2018) 1–21, https://doi.org/10.3390/su10010086.
[48] N. Dabuth, S. Thuangchon, T. Prasert, V. Yuthawong, P. Phungsai, Effects of catalytic ozonation catalyzed by TiO_2 activated carbon and biochar on dissolved organic matter removal and disinfection by-product formations investigated by

Orbitrap mass spectrometry, J. Environ. Chem. Eng. 10 (2022) 107215, https://doi.org/10.1016/j.jece.2022.107215.
[49] C.M. Morrison, S. Hogard, R. Pearce, D. Gerrity, U. von Gunten, E.C. Wert, Ozone disinfection of waterborne pathogens and their surrogates: a critical review, Water Res 214 (2022) 118206, https://doi.org/10.1016/j.watres.2022.118206.
[50] H.E. Al-hazmi, H. Shokrani, A. Shokrani, K. Jabbour, O. Abida, S. Soroush, M. Khadem, S. Habibzadeh, S.H. Sonawane, Recent advances in aqueous virus removal technologies, Chemosphere 305 (2022), https://doi.org/10.1016/j.chemosphere.2022.135441.